Dyes and Pigments 113 (2015) 664–674

Contents lists available at ScienceDirect

Dyes and Pigments

journal homepage: www.elsevier.com/locate/dyepig

Review

New luminophors based on the binuclear helicates of *d*-METALS with BIS(DIPYRRIN)S

Elena V. Antina [a], Rimma T. Kuznetsova [b], Lubov A. Antina [a], Galina B. Guseva [a], Natalia A. Dudina [a, *], Anatolij I. V'yugin [a], Alexey V. Solomonov [c]

[a] G.A. Krestov Institute of Solution Chemistry of Russian Academy of Sciences (ISC RAS), 1 Akademicheskaya st., 153045, Ivanovo, Russian Federation
[b] Siberian Physical-Technical Institute of Tomsk State University, 1 Novosobornaya sq., 634050, Tomsk, Russian Federation
[c] Inorganic Chemistry Department, Ivanovo State University of Chemistry and Technology (ISUCT), 7 Sheremetevskij prosp., 153000, Ivanovo, Russian Federation

ARTICLE INFO

Article history:
Received 22 July 2014
Received in revised form
1 October 2014
Accepted 5 October 2014
Available online 12 October 2014

Keywords:
Bis(dipyrrin)s
Binuclear homoleptic double–helical complexes
Photonics
Sensors of medium polarity
Spectral-luminescent properties
Lasing characteristics

ABSTRACT

The review highlights recent advances devoted to new luminophores based on *d*-metal complexes of bis(dipyrrin)s of $[M_2L_2]$. The $[M_2L_2]$ helicates possess intense absorption in a visible spectrum region. The $[Zn_2L_2]$, $[Cd_2L_2]$ and $[Hg_2L_2]$ helicates are fluorophores with the most intense fluorescence in nonpolar solvents. The fluorescence of $[M_2L_2]$ bis(dipyrrinate)s decreases by two-fold in aromatic solvents and becomes close to zero in electron-donor media. The fluorescence is increased in a series of 2,2′-, 2,3′-, 3,3′-bis(dipyrrinate)s with similar complexing agent and in a series of $[Hg_2L_2]$, $[Cd_2L_2]$, $[Zn_2L_2]$ complexes with the same ligand. Upon freezing and cooling of $[Zn_2L_2]$ in ethanol from 300 to 77 K the fluorescence quantum yield of $[Zn_2L_2]$ is increased up to 100 times. The $[Zn_2L_2]$ complexes are able to generate the stimulated emission induced at the 550–560 nm region in nonpolar solvents upon excitation by second harmonic Nd:YAG laser.

© 2014 Elsevier Ltd. All rights reserved.

1. Introduction

The significance of mononuclear homoleptic complexes of dipyrrins in respect to the study of coordination chemistry became apparent not long after their initial discovery [1]. This family of compounds is based on the dipyrrinato (*bis*-pyrrolic) monoanionic chelating derivatives (Fig. 1). Since their discovery and particularly over the past two decades, 4,4-difluoro-4-bora-3a,4a-diaza-*s*-indacene, boron dipyrromethene derivative (BODIPY) (boron dipyrromethene complex, Fig. 1) have emerged as a fascinating class of dyes with excellent performance and stability. Thereby, these compounds have found application in sensing, labelling, light-harvesting technologies and photodynamic therapy [2–11].

For a long time it was considered that homoleptic dipyrrinato metal complexes were incapable to fluorescence, in contrast to their highly fluorescent boron-dipyrrinato analogues. But in the 1987 it was reported that the Zn(II) dipyrrinato complex, prepared from *meso*-unsubstituted dipyrrine, is highly fluorescent with fluorescence quantum yield $\Phi_f = 0.048 \pm 0.012$ in a binary mixture of toluene:chloroform (100:1). Very encouraging results were obtained using of *meso*-unsubstituted Zn(II) dipyrrinates as sensitizers of singlet oxygen [12].

In most other studies *meso*-aryl-substituted dipyrrinates of metals were used. For example, an addition of *meso*-phenyl- and *meso*-(4-*tert*-butylphenyl-) substitutions results in very weak emission with rapidly deactivating excited state lifetimes as seen for compounds **3** and **4** in Fig. 2. Only in 2004 it was reported that the Zn(II)-dipyrrinato complex **5** (Fig. 2), prepared from 5-mesityldipyrrin, was highly fluorescent with multinanosecond singlet excited state lifetime [13]. Homoleptic Ga(III) and In (III) analogues of **5** exhibit less intense fluorescence (Φ_f in hexanes 0.024 and 0.074 respectively) [14].

Presumably the 2,6-methyl fragments of the mesityl group in 5 prohibit internal rotation and such steric constraints drastically enhance the excited state lifetime of complexes involving 5-mesityldipyrrinato ligands. These properties are of interest in applications whereby intense absorption and fluorescence attributes in the visible region are desirable.

* Corresponding author.
E-mail addresses: eva@isc-ras.ru (E.V. Antina), kuznetrt@phys.tsu.ru (R.T. Kuznetsova), lyubov.antina@mail.ru (L.A. Antina), gbg@isc-ras.ru (G.B. Guseva), nad@isc-ras.ru (N.A. Dudina), aiv@isc-ras.ru (A.I. V'yugin), Deus-Lex@yandex.ru (A.V. Solomonov).

http://dx.doi.org/10.1016/j.dyepig.2014.10.002
0143-7208/© 2014 Elsevier Ltd. All rights reserved.

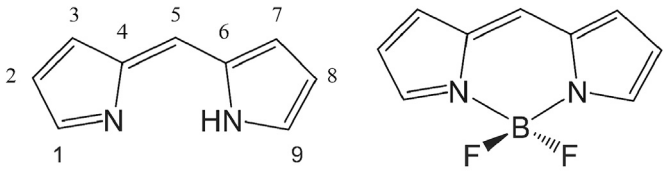

Dipyrrin (**1**) Boron dipyrromethene complex (**2**)

Fig. 1. Structure of dipyrrin **1** and 4,4-difluoro-4-bora-3a,4a-diaza-*s*-indacene (boron dipyrromethene complex) **2**.

Further this hypothesis was confirmed in an independent study of the dimeric $[Zn(dipyrrin)Cl]_2$ species such as **6** and **7** (Fig. 3) [15,16]. In these compounds, formed by self-assembly, the Zn(II)-cation is coordinated to the dipyrrin chelate and the rotation of pyridyl group, relative to the dipyrrinato unit, is prohibited.

Promising results from a study of B(III) and Zn(II) dipyrrinates luminescent properties laid the foundation of open-chain oligopyrrole coordination compounds in photonics. At the present time two main areas of influence on the fluorescence of dipyrrin luminophors are developed. The first using a new type of ligands with higher rigidity of molecules (N_2O_2-type [17–21] and N_3-type [22]), and the second varies the nature of the complexing agent (*d*- and *f*-metals [13,15,16,23], Ga(III) and In(III) [14,24], B(III) [25–28], Al(III), [18] Si(IV)) [29].

Bis(dipyrrin)s chemistry began actively growing at the beginning of the XXI century [23,30–36]. Bis(dipyrrin)s are the open-chain tetrapyrrolic ligands (H_2L), which are constructed from two chromophore dipyrrin domains linked by spacer at the 2,2′-, 2,3′- or 3,3′-positions of proximal pyrroles (**8**–**10** in Fig. 4).

The bis(dipyrrin)s as tetradentate N_4-ligands are able to form a mono-, bi- or polynuclear coordination compounds with divalent or trivalent ions of a number of *p*-, *d*- and *f*-elements with different composition and structure including porphyrin-like [ML] [37–39], double helical $[M_2L_2]$ [23,31,34–36], triple-stranded $[M_2L_3]$ [33,40,41], triangle $[M_3L_3]$ [42], [2 × 2] grids $[M_4L_4]$ [43] and hexagon $[M_6L_6]$ [43] (schematic structures in Fig. 5). Polynuclear complexes are of greatest interest because of the intense chromophore properties ($\varepsilon \geq 10^5$ L mol^{-1} cm^{-1}). Binuclear double-helicates are the most stable of them [23,31,34–36,44].

Well-known 2,2′-bis(dipyrrin)s – biladiene-*a*,*c* derivatives form both mononuclear porphyrin-like complexes and binuclear

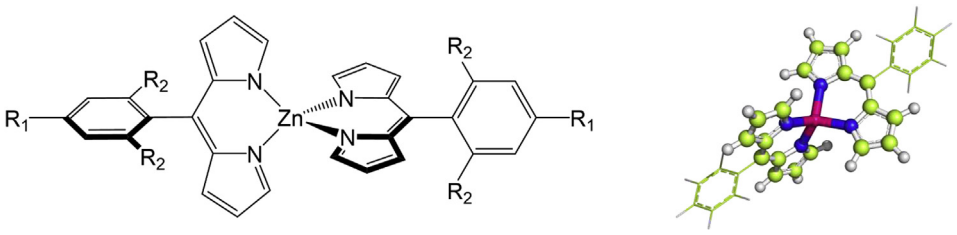

A B

3 R_1, R_2 = H; **4** R_1 = 4-*tert*-butyl (^{t}Bu), R_2 = H; Φ_f = 0.006, λ_{em} = 501 nm (toluene);

5 R_1, R_2 = CH_3; Φ_f = 0.36, λ_{em} = 500 nm (toluene)

Fig. 2. Schematic (A) and general molecular structure (B) of nonfluorescent (**3** and **4**) and fluorescent (**5**) Zn(II)-dipyrrinato complexes.[13,14].

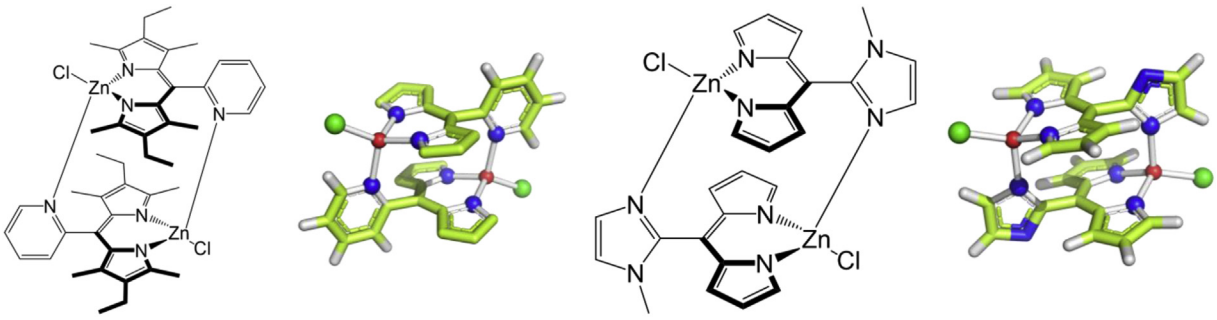

6; Φ_f =0.057, λ_{em} = 523 nm (methylene chloride) **7**; Φ_f =0.013, λ_{em} = 632 nm (chloroform)

Fig. 3. Luminescent dimeric $[Zn(dipyrrin)Cl]_2$ complexes. Several H atoms and peripheral groups are omitted for clarity [15,16].

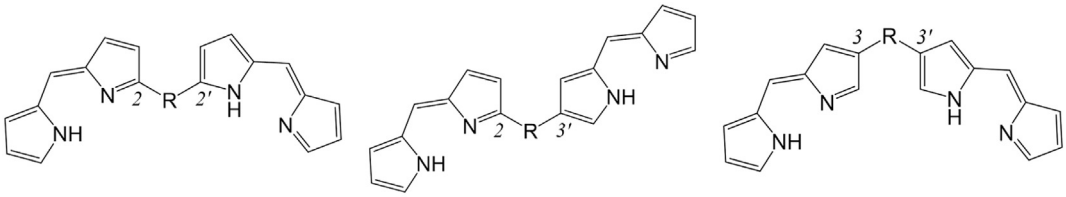

8 2,2'-bis(dipyrrin) **9** 2,3'-bis(dipyrrin) **10** 3,3'-bis(dipyrrin)

Fig. 4. Structural variations of bis(dipyrrin)s.[23].

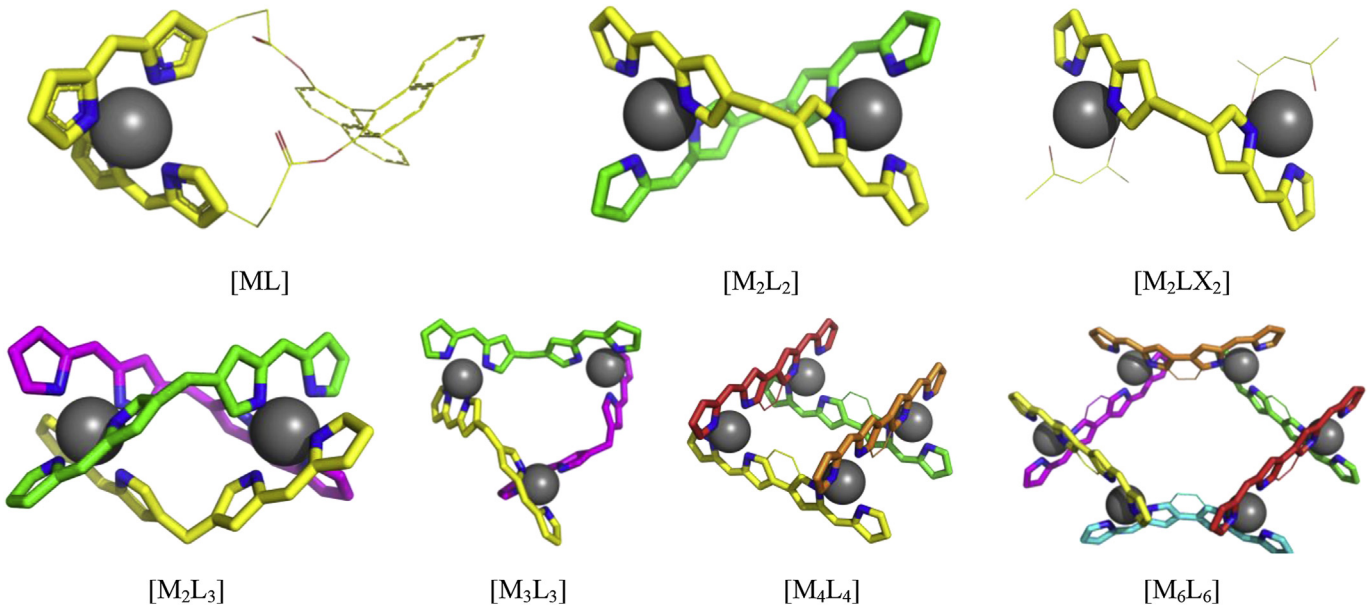

Fig. 5. Typical structures of 3,3′-bis(dipyrrin) complexes: [ML] – mononuclear complex [37–39]; [M_2L_2] – binuclear double helical complex [23,31,34–36]; [M_2LX_2] – binuclear heteroleptic complex (X – any other ligand); [M_2L_3] – binuclear triple-stranded helicate [33,40,41]; [M_3L_3] – trinuclear molecular triangle [42]; [M_4L_4] – [2 × 2] grids [43]; [M_6L_6] – hexagon structure (six-core molecular hexagon) [43]. ● – metal ion. H atoms and peripheral groups are omitted for clarity. Coordination core is tetrahedron.

helicates [39]. Recently, the 2,3′- and 3,3′-analogues with improved preorganization (especially, the latter) by changing the position of the spacer, capable to formation of stable binuclear structures, were obtained [31,32,44,45].

Over the past 10 years, some helicates of *d*-and *f*-metals with 2,3′- and 3,3′-bis(dipyrrin) derivatives, having different molecular structure, including the nature of central spacer and the functional substituents, were synthesized [23,44–51]. The high practical potential of dipyrrinates in terms of the construction of supramolecular light-harvesting structures was confirmed [10].

The review highlights the results of our studies of new luminophores based on *d*-metal complexes of bis(dipyrrin)s [44–55].

2. Spectral-luminescent, photochemical, lasing characteristics and other physico-chemical properties of bis(dipyrrin) helicates

The synthesis and X-ray diffraction analysis of a series [M_2L_2] binuclear homoleptic helicates of Co(II), Ni(II), Cu(II), Zn(II), Cd(II) and Hg(II) with 3,3′-, 2,3′- and 2,2′-bis(dipyrrin)s having central methylene, aryl- or trifluoromethylene-methylene spacers in its structure and different numbers of methyl and ethyl substituents (from 4 to 10) in the pyrrolic rings of ligands (compounds [M_2(**11**)$_2$]–[M_2(**21**)$_2$] are presented in Fig. 6) [46–51] were carried out. The electronic absorption spectra of [M_2L_2] in different solvents [44,46–51], the lability of helicates in proton-donor media [52] and the thermal stability of helicates in the solid phase [44,45] were investigated.

A very strong fluorescence of Zn(II), Cd(II) and Hg(II) helicates [M_2L_2] was detected [44,47,48,50,51] which was surprising because the luminescent properties of [M_2L_2] had not been previously explored. Due to this, we began work on the study of photonics of [M_2L_2] helicates.

The data on the absorption and fluorescence spectra, generation stimulated emission, phosphorescence, fluorescence quantum yields (Φ_f) and phototransformations (Φ_{photo}), fluorescence lifetimes (τ) of long-lived radiation, radiation constants (k_{rad}) of complexes [M_2(**11**)$_2$]–[M_2(**21**)$_2$] in different solvents, binary mixtures and in frozen solutions are summarized in Tables 1–5 [44,46–51,53–55].

2.1. Electronic absorption spectra

Characteristics of electronic absorption spectra of helicates [M_2(**11**)$_2$]–[M_2(**21**)$_2$] in organic solvents are presented in Tables 1–4 [44,46–51]. As seen from Tables 1–4 and Fig. 7, the absorption spectra contain three bands caused by S^0–S^n electronic transitions. The λ^{abs}_{max} for the most intense S^0–S^1 and S^0–S^2 bands lies in the range 503–551 nm and 460–495 nm, respectively, depending on the metal and ligand nature [44,46–51]. Low-intensity broadened S^0–S^3 band appears in the range from 330 to 380 nm.

In the spectra of [Zn_2L_2], [Cd_2L_2], [Hg_2L_2] and [Co_2L_2] helicates the first and the second bands are strongly overlapped and the ratio of intensities of the bands has the form $\lambda^1_{max} > \lambda^2_{max} \gg \lambda^3_{max}$ (Fig. 7(A)).

In the [Ni_2L_2] and [Cu_2L_2] spectra, the first and the second bands are overlapped less, and S^0–S^2 band is the most intense in spectrum of [Cu_2L_2] solutions (Fig. 7(B)). lgε values of intense bands in the [M_2L_2] spectra reaches 4.84–5.49 as for the Soret band in the absorption spectra of porphyrins [56].

An addition of $-PhOCH_3$ and $-CF_3$ groups to *meso*-spacer of ([Zn_2(**18**)$_2$] and [Zn_2(**19**)$_2$], respectively) and especially the transfer of *meso*-spacer from 3,3′- to 2,3′- and 2,2′-position ([Zn_2(**20**)$_2$] and [Zn_2(**21**)$_2$], respectively) causes lgε value reduction of intense band in the [M_2L_2] spectrum (see Tables 1 and 3).

It should also be noted that λ^1_{max} and λ^2_{max} are shifted (~30 nm) to the red region in the absorption spectrum of 3,3′-bis(dipyrrinate)s compared to 2,2′-bis(dipyrrinate)s or mononuclear [$M(dpm)_2$] dipyrrinates [13]. For example, a substitution of 3,3′- or 2,3′- on 2,2′-bis(dipyrrin) causes significant hypsochromic shift (~20 nm) and intensity (λ^1_{max} of the S^0–S^2 band) decreasing in the biladiene [Zn_2(**21**)$_2$] complex spectrum compared to [Zn_2(**11**)$_2$] and [Zn_2(**20**)$_2$] analogues (see Tables 1 and 3).

The influence of metal cation on the dye spectrum (auxochromic effect) can be calculated as difference between the wavelengths of intensity maxima band in absorption spectra of the complex and the ligand:

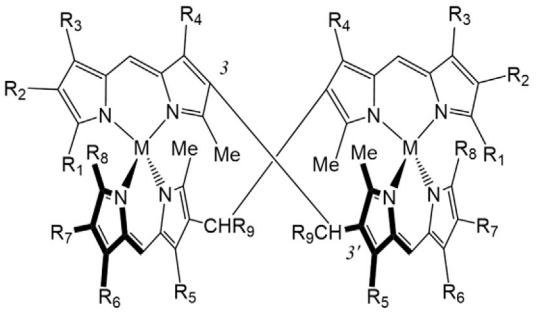

$[M_2L_2]$ (M = Co^{2+}, Ni^{2+}, Cu^{2+}, Zn^{2+}, Cd^{2+} and Hg^{2+})

$[M_2(\mathbf{11})_2]$: R_1=R_2=R_3=R_4=R_5=R_6=R_7=R_8=Me; R_9=H

$[M_2(\mathbf{12})_2]$: R_1=R_3=R_4=R_5=R_6=R_8=Me; R_2=R_7=Et; R_9=H

$[Zn_2(\mathbf{13})_2]$: R_1=R_3=R_4=R_5=R_6=R_8=Me; R_2=R_7=Et; R_9=Ph

$[Zn_2(\mathbf{14})_2]$: R_1=R_2=R_3=R_6=R_7=R_8=Me; R_4=R_5=Et; R_9=H

$[Zn_2(\mathbf{15})_2]$: R_1=R_3=R_4=R_5=R_6=R_8=Me; R_2=R_7=R_9=H

$[Zn_2(\mathbf{16})_2]$: R_2=R_3=R_4=R_5=R_6=R_7=Me; R_1=R_8=R_9=H

$[Zn_2(\mathbf{17})_2]$: R_4=R_5=Me; R_1=R_2=R_3=R_6=R_7=R_8=R_9=H

$[Zn_2(\mathbf{18})_2]$: R_1= R_2=R_3=R_4=R_5=R_6=R_7=R_8=Me; R_9=PhOMe

$[Zn_2(\mathbf{19})_2]$: R_1= R_2=R_3=R_4=R_5=R_6=R_7=R_8=Me; R_9=CF_3

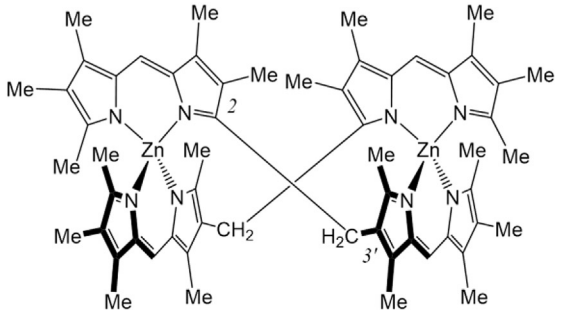

$[Zn_2(\mathbf{20})_2]$

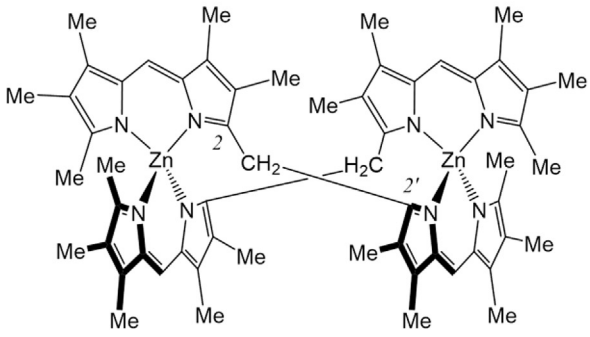

$[Zn_2(\mathbf{21})_2]$

Fig. 6. Structures of binuclear homoleptic $[M_2L_2]$ helicates [46–51].

Table 1
Spectral-luminescent characteristics of the $[Zn_2L_2]$ complex in organic solvents [44,47,48].

Compound	Solvent	λ^{abs}_{max}, lgε (S^0–S^1); (S^0–S^2); (S^0–S^3)[a]	$\lambda^{fl}_{max}(\lambda_{ex})$[a]	$\Delta\nu_{St}$[b]	Φ_f[c]	$k_{rad}\cdot10^{-8}$[d]	τ[e]
$[Zn_2(\mathbf{11})_2]$	Cyclohexane	530, 5.40; 478, 4.96; 370, 4.27	543	452	0.91	2.7	3.3
	Benzene	530, 5.48; 478, 5.08; 369, 4.31	545	519	0.56	3.2	1.7
	Hexane	527, 5.47; 478, 5.07; 367, 4.52	541	491	0.61	3.8	1.6
	Heptane	527, 5.47; 478, 5.05; 366, 4.32	542	525	0.66	3.5	1.9
	Toluene	531, 5.46; 481, 5.06; 377, 4.33	545	484	0.64	3.2	2.0
	Tetrahydrofuran	528, 5.46; 478, 5.05; 365, 4.38	542	489	0.13	3.4	0.38
	Chloroform	529, 5.43; 479, 5.09; 369, 4.36	544	521	0.025	3.4	0.074
	1-propanol	527, 5.40; 477, 4.99; 367, 4.25	542	525	0.010	3.3	0.027
	Ethanol	525, 5.44; 476, 5.04; 370, 4.27	542	597	0.005	3.7	0.013
	Dimethylformamide	526, 5.34; 477, 4.94; 367, 4.22	543	595	0.002	2.8	0.007
	Dimethyl sulfoxide	527; 478; 381	–	–	0.000	–	–
	Pyridine	531; 480; 363	549	617	0.010	–	–
	Ethyl acetate	526; 479; 369	546	697	0.003	–	–
	Acetone	524; 476; 360	541	600	0.003	–	–
	Acetonitrile	523; 476; 365	–	–	0.000	–	–
$[Zn_2(\mathbf{12})_2]$	Cyclohexane	531, 5.49; 479, 5.08; 368, 4.30	545 (495)	484	0.77	3.2	2.4
	Dimethylformamide	526, 5.42; 478, 5.03; 360, 4.29	542 (495)	561	0.003	3.5	0.006
$[Zn_2(\mathbf{13})_2]$	Cyclohexane	530, 5.47; 480, 5.14; 370, 4.31	547 (495)	586	0.70	4.0	1.8
	Dimethylformamide	527, 5.45; 479, 5.13; 356, 4.33	546 (495)	660	0.003	4.2	0.007
$[Zn_2(\mathbf{14})_2]$	Cyclohexane	529, 5.37; 480, 4.97; 369, 4.18	543 (495)	487	0.83	2.7	3.04
	Dimethylformamide	526, 5.33; 479, 4.96; 357, 4.27	543 (495)	595	0.002	2.9	0.007
$[Zn_2(\mathbf{15})_2]$	Cyclohexane	523; 471; 354–363	534 (485)	399	0.96	–	–
	Dimethylformamide	519, 5.47; 470, 5.06; 370, 4.32	532 (490)	471	0.003	3.9	0.008
$[Zn_2(\mathbf{16})_2]$	Cyclohexane	525; 474; 370–380	536 (485)	391	0.83	–	–
	Dimethylformamide	521, 5.32; 473, 4.87; 375, 4.28	535 (490)	502	0.004	3.2	0.013
$[Zn_2(\mathbf{17})_2]$	Cyclohexane	509; 459; 348	520 (480)	416	0.94	–	–
	Dimethylformamide	503, 5.30; 457, 4.87; 357, 4.19	518 (480)	576	0.004	3.3	0.012
$[Zn_2(\mathbf{18})_2]$	Cyclohexane	531; 480; 365	547 (495)	531	0.59	–	–
	Dimethylformamide	524, 5.27; 480, 5.04; 371, 4.35	545 (495)	735	0.002	4.4	0.005
$[Zn_2(\mathbf{19})_2]$	Cyclohexane	524, 5.28; 474, 5.02; 366, 4.21	541 (490)	600	0.43	–	–
	Dimethylformamide	519, 5.24; 472, 4.97; 369, 4.19	539	715	0.002	3.2	0.006

[a] λ^{abs}_{max}, λ_{ex} (495 nm) and λ^{fl}_{max} – absorption, excitation and fluorescence maxima, respectively, nm; ε – molar absorption coefficient (L mol^{-1} cm^{-1}). Ref. [44,47,48].
[b] $\Delta\nu_{St}$ – Stokes shift (cm^{-1}). Ref. [44,47,48].
[c] Φ_f – fluorescence quantum yield. Ref. [44,47,48].
[d] k_{rad} – radiation constant (s^{-1}). Ref. [44,47,48].
[e] τ – fluorescence lifetime (ns). Ref. [44,47,48].

Table 2
Spectral-luminescent characteristics of the $[Cd_2(\mathbf{11})_2]$ and $[Hg_2(\mathbf{11})_2]$ complexes in organic solvents [44,50,51].

Compound	Solvent	λ^{abs}_{max}, nm, lgε (S^0–S^1); (S^0–S^2); (S^0–S^3)[a]	λ^{fl}_{max}[a]	$\Delta\nu_{St}$[b]	Φ_f[c]
$[Cd_2(\mathbf{11})_2]$	Cyclohexane	525; 475; 362	537	426	0.21
	Benzene	526, 5.40; 477, 4.98; 367, 4.30	540	493	0.12
	Hexane	521; 475; 356	535	502	0.16
	1-propanol	521; 474; 377	534	467	0.012
	Ethanol	519; 473; 373	534	541	0.005
	Dimethylformamide	521, 5.37; 475, 4.95; 362, 4.28	539	641	0.003
$[Hg_2(\mathbf{11})_2]$	Cyclohexane	524; 476; 365	538	497	0.034
	Benzene	524; 479; 369	540	565	0.003
	Hexane	521; 476; 367	536	537	0.025
	1-propanol	519; 477; 383	535	576	0.002
	Ethanol	516; 477; 380	533	618	0.001

*For $[Cd_2(\mathbf{11})_2]$ in benzene $k_{rad} = 3.3\cdot10^{-8}$ s^{-1} and $\tau = 0.37$ ns.
[a] λ^{abs}_{max}, λ_{ex} (495 nm) and λ^{fl}_{max} – absorption, excitation and fluorescence maxima, respectively, nm; ε – molar absorption coefficient (L mol^{-1} cm^{-1}). Ref. [44,50,51].
[b] $\Delta\nu_{St}$ – Stokes shift (cm^{-1}). Ref. [44,50,51].
[c] Φ_f – fluorescence quantum yield. Ref. [44,50,51].

$$\Delta\lambda^{M^{2+}} = \lambda^{[M_2L_2]} - \lambda^{H_2L}.$$

The value of $\Delta\lambda$ increases from 36 to 91 nm in the following series of complexing ions: Cu(II) < Hg(II) ≤ Cd(II) < Zn(II) ≤ Co(II) < Ni(II) (Fig. 8(A)). Decrease of the alkyl substituents count leads to $\Delta\lambda$ increasing [44]. For example, for $[Zn_2(\mathbf{11})_2]$–$[Zn_2(\mathbf{15})_2]$ $\Delta\lambda$ = 63–70 nm, for $[Zn_2(\mathbf{16})_2]$ and $[Zn_2(\mathbf{17})_2]$ complexes with either partially (at α-positions) or completely unsubstituted terminal pyrroles, the values of $\Delta\lambda$ increases to 75 and 88 nm, respectively (Fig. 8(B)).

Table 5
Lasing, photochemical and resource characteristics of laser media based on the $[Zn_2L_2]$ cyclohexane solutions upon excitation by the second harmonic of Nd:YAG laser.[53–55].

Compound	Concentration 10^{-4}, M	W_{pump}[a]	Efficiency, %	λ_{gen}[b]	Φ_{photo} $10^{-5}\pm$ 10%[c]	P_{80}[d]
$[Zn_2(\mathbf{11})_2]$	1.0	15	3.4	557	2.0	33
$[Zn_2(\mathbf{11})_2]$	2.0	15	6.9	561	23	75
$[Zn_2(\mathbf{12})_2]$	1.0	15	5.1	557	4.0	43
$[Zn_2(\mathbf{12})_2]$	2.0	10	10	559	10	80
		25	10	560	9.0	120
$[Zn_2(\mathbf{14})_2]$	1.0	15	3.3	555	2.0	60
$[Zn_2(\mathbf{14})_2]$	2.0	10	11	561	7.3	80

[a] W_{pump}, MW × cm^{-2} – pump density. Ref. [53–55].
[b] λ_{gen}, nm – lasing wavelength of stimulated emission. Ref. [53–55].
[c] Φ_{photo} – quantum yield of phototransformations. Ref. [53–55].
[d] P_{80}, J × cm^{-3} – resource of laser media. Ref. [53–55].

The addition electron withdrawing $-CF_3$ groups to 3,3′-spacer of a helicand which gives a hypsochromic shift (to 7 nm) of the S^0–S^1 band maximum in the absorption spectrum of $[Zn_2(\mathbf{19})_2]$, compared to unsubstituted analogue $[Zn_2(\mathbf{11})_2]$.

Solvatochromism is detected as a small bathochromic shift (up to 6 nm) and as increasing of intensity of bands in the $[M_2L_2]$ helicates spectra in nonpolar and weakly polar solvents (hexane, heptane, benzene, toluene) compared to polar media (1-propanol, ethanol, chloroform, and dimethylformamide).

2.2. Photonics of $[M_2L_2]$ helicates and its application perspectives

2.2.1. Effects of helicate structure

$[Co_2L_2]$, $[Ni_2L_2]$, and $[Cu_2L_2]$ complexes are not fluorophores [49–51]. $[M_2L_2]$ helicates, formed by Zn^{2+}, Cd^{2+} and Hg^{2+} ions

Table 3
Spectral-luminescent characteristics of the $[Zn_2(\mathbf{20})_2]$ and $[Zn_2(\mathbf{21})_2]$ complexes in organic solvents [46].

Compound	Solvent	λ^{abs}_{max}, nm, lgε (S^0–S^1); (S^0–S^2); (S^0–S^3)[a]	λ^{fl}_{max}[a]	$\Delta\nu_{St}$[b]	Φ_f[c]	$k_{rad}\cdot10^{-8}$[d]	τ[e]
$[Zn_2(\mathbf{20})_2]$	Cyclohexane	529; 476; 367	537	282	0.39	–	–
	Benzene	530, 5.24; 479, 5.07; 368, 4.32	547	586	0.060	2.0	0.30
	Hexane	527; 475; 373	537	353	0.35	–	–
	Heptane	528; 476; 360	536	283	0.27	–	–
	Toluene	530, 5.23; 479, 5.07; 370, 4.30	547	586	0.080	2.0	0.40
	Tetrahydrofuran	527; 477; 368	548	727	0.13	–	–
	Ethanol	526; 476; 373	547	730	0.001	–	–
	Dimethylformamide	527, 5.20; 476, 4.98; 367, 4.27	561	1150	0.007	2.2	0.032
$[Zn_2(\mathbf{21})_2]$	Cyclohexane	510; 467; 373	549	1393	0.036	–	–
	Benzene	514, 5.11; 471, 5.09; 375, 4.30	551	1306	0.018	2.5	0.071
	Hexane	510; 467; 375	549	1393	0.024	–	–
	Heptane	510; 468; 374	550	1426	0.026	–	–
	Toluene	515, 5.09; 472, 5.07; 375, 4.30	552	1302	0.021	2.3	0.093
	Tetrahydrofuran	511, 5.03; 468, 5.02; 376, 4.15	551	1421	0.011	2.1	0.053
	Chloroform	513, 5.06; 469, 5.04; 380, 4.26	549	1278	0.005	2.3	0.022
	Dimethylformamide	511; 470; 380	–	–	0.000	–	–

[a] λ^{abs}_{max}, λ_{ex} (495 nm) and λ^{fl}_{max} – absorption, excitation and fluorescence maxima, respectively, nm; ε – molar absorption coefficient (L mol^{-1} cm^{-1}). Ref. [46].
[b] $\Delta\nu_{St}$ – Stokes shift (cm^{-1}). Ref. [46].
[c] Φ_f – fluorescence quantum yield. Ref. [46].
[d] k_{rad} – radiation constant (s^{-1}). Ref. [46].
[e] τ – fluorescence lifetime (ns). Ref. [46].

Table 4
Quantitative characteristics (λ^{abs}_{max}, nm; lgε) of electronic absorption spectra of the $[Co_2(\mathbf{11})_2]$, $[Ni_2(\mathbf{11})_2]$ and $[Cu_2(\mathbf{11})_2]$ complexes in organic solvents [49–51].

Solvent	Compound		
	$[Co_2(\mathbf{11})_2]$	$[Ni_2(\mathbf{11})_2]$	$[Cu_2(\mathbf{11})_2]$
Cyclohexane	529; 492; 376	551; 464; 395	538; 495; 397
Benzene	530, 5.08; 495, 4.75; 377, 4.30	553, 4.84; 464, 4.60; 395, 4.47	539, 4.91; 496, 5.04; 392, 4.28
Chloroform	528, 5.08; 494, 4.77; 377, 4.32	551, 4.88; 461, 4.62; 396, 4.48	536, 4.90; 497, 5.03; 390, 4.24
Dimethylformamide	526, 5.09; 494, 4.76; 377, 4.32	547, 4.84; 460, 4.60; 396, 4.46	535, 4.85; 492, 5.01; 386, 4.26

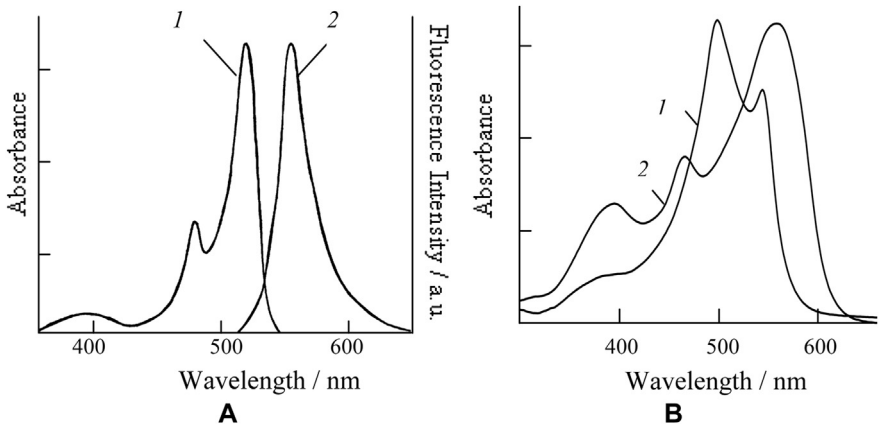

Fig. 7. Normalized electronic absorption (*1*) and emission (*2*) spectra (λ_{ex} = 495 nm) of [Zn_2(**11**)$_2$] complex in benzene (A); electronic absorption spectra of [Cu_2(**11**)$_2$] (*1*) solutions ($c = 3.37 \times 10^{-5}$ M) and [Ni_2(**11**)$_2$] (*2*) complexes ($c = 3.59 \times 10^{-5}$ M) in benzene (B) [44,49,50].

with external filled d^{10}-sublayer, have intense fluorescence in saturated and aromatic hydrocarbons [44,47,50,51] (see Tables 1–3). The emission spectra of [Zn_2L_2], [Cd_2L_2] and [Hg_2L_2] complexes are the mirror images of the absorption spectra (see Fig. 7(A), example for Zn(II) complex). The Stokes shift ($\Delta\nu_{St}$) for 3,3′-bis(dipyrrinate)s and 2,3′-bis(dipyrrinate)s is 391–735 and 282–1150 cm^{-1}, respectively, and much less than that for the 2,2′-bis(dipyrrinate)s (1278–1426 cm^{-1}). Addition of substituents to the central *meso*-spacer causes an increase of $\Delta\nu_{St}$ for complexes [Zn_2(**13**)$_2$], [Zn_2(**18**)$_2$], [Zn_2(**19**)$_2$] compared to unsubstituted analogues [Zn_2(**11**)$_2$] and [Zn_2(**12**)$_2$]. The values of radiation constants (k_{rad}) are sufficiently high (from 2.0×10^8 to 4.35×10^8 s^{-1}) and have weak dependence on the solvent nature (see Tables 1–3) [53].

Changing 3,3′-bis(dipyrrinate) fragments onto 2,3′- and especially 2,2′-bis(dipyrrinate)s causes decreasing of fluorescence quantum yield of [Zn_2L_2] complexes. For instance, in cyclohexane Φ_f for [Zn_2(**11**)$_2$], [Zn_2(**20**)$_2$] and [Zn_2(**21**)$_2$] equals to 0.91, 0.39 and 0.036, respectively. Probably the reason for the strong influence of the spacer position is significant differences in radiation constants (k_{rad}), which for [Zn_2(**20**)$_2$] and [Zn_2(**21**)$_2$] is less than [Zn_2(**11**)$_2$] (see Tables 1 and 3). Herewith, the quantum yield of triplet molecules could be correspondingly higher.

The differences in the alkyl substitution of the pyrrole rings of the ligands have no significant impact on the value of Φ_f for the complexes with methylene 3,3′-spacer in helicands. The addition of –Ph, –PhOMe and $-CF_3$ groups to the *meso*-spacer causes a slight decrease of Φ_f for the [Zn_2(**13**)$_2$], [Zn_2(**18**)$_2$] and [Zn_2(**19**)$_2$] complexes.

2.2.2. *Influence of the solvent nature*

Influence of the solvent properties (see Tables 1–3) was studied in detail using ([Zn_2(**11**)$_2$]–[Zn_2(**21**)$_2$], [Cd_2(**11**)$_2$] and [Hg_2(**11**)$_2$]) complexes [44,53]. The Φ_f values is 0.54–0.99 for [Zn_2L_2] complexes with 3,3′-bis(dipyrrin)s in nonpolar and weakly polar saturated and aromatic hydrocarbons. For most Zn(II), Cd(II) and Hg(II) helicates the maximum value of Φ_f (the excitation wavelength λ_{ex} = 485–495 nm) is observed in cyclohexane. For example, for the [Zn_2(**11**)$_2$], [Zn_2(**15**)$_2$], [Zn_2(**17**)$_2$] complexes values of Φ_f are 0.91–0.96 in cyclohexane (Fig. 9(A)). Under similar conditions the medium value of Φ_f more than two times lower for the Cd(II) complexes and an order of magnitude lower for the [Hg_2(**11**)$_2$] complex compared with [Zn_2L_2] (Fig. 9(B)).

The tendency of fluorescence quenching of [Zn_2L_2] and [Cd_2L_2] helicates in aromatic solvents compared to saturated hydrocarbons is very noticeable [44,53]. The Φ_f value decreases by ~2.5 times for 3,3′- and 2,2′-bis(dipyrrinate)s [Zn_2(**11**)$_2$], [Zn_2(**12**)$_2$], [Zn_2(**14**)$_2$]–[Zn_2(**17**)$_2$] complexes and ~7 times for 2,3′-bis(dipyrrinate) [Zn_2(**20**)$_2$] in toluene and benzene in comparison with hexane, heptane and cyclohexane. The reason for this decrease is the increase of chromophore molecules solvation (π–π stacking) in the excited state, which creates prerequisites for using of complexes as fluorescent sensors of aromatic compounds.

A dramatic fluorescence quenching of [M_2L_2] in chloroform and electron-donating solvents (Tables 1–3) is observed. The fluorescence lifetime (τ) of the [Zn_2L_2] helicates increases from ~0.007 to ~3 ns with decreasing of solvent polarity. This fact confirms a significant role of solvation shell during the excitation energy deactivation process.

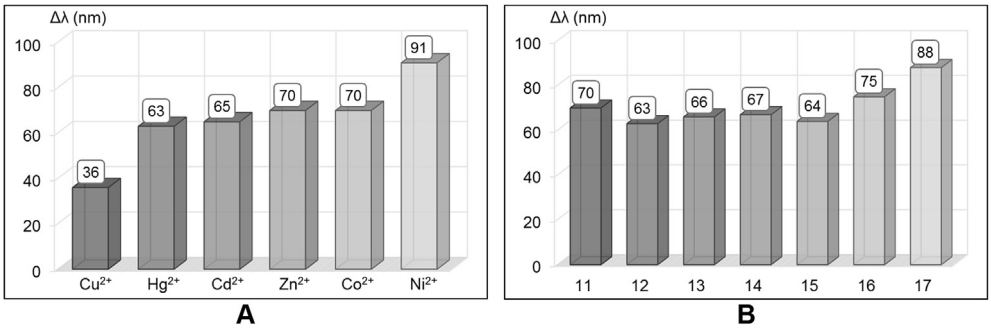

Fig. 8. Auxochromic effect ($\Delta\lambda^{M^{2+}} = \lambda^{[M_2L_2]} - \lambda^{H_2L}$, nm) of M^{2+} ions in [M_2(**11**)$_2$] complex (A) and auxochromic effect of Zn^{2+} cation in [Zn_2(**11**)$_2$]–[Zn_2(**17**)$_2$] complexes (B) according to the electronic absorption spectra of compounds in DMF [44]. Values of $\lambda^{1}_{H_2L}$ in dimethylformamide were taken from paper.[57].

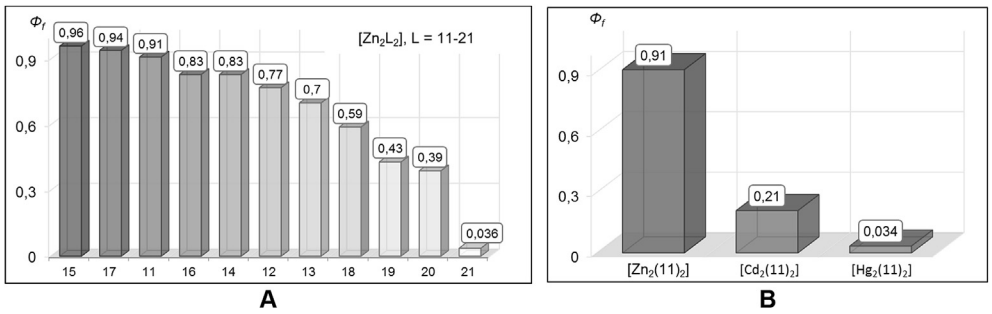

Fig. 9. The fluorescence quantum yield (Φ_f) of $[Zn_2L_2]$ complexes in cyclohexane depending on the nature of ligand (A) and complexing ion (B) [44,53].

Dependences of $\Delta\nu_{St}$ values on the universal interaction function Δf (parameter of solvents polarity) are nonlinear for Zn(II), Cd(II) and Hg(II) helicates. For example, the dependence of $\Delta\nu_{St}$ on Δf for $[Zn_2(\mathbf{11})_2]$ has two separate areas for nonpolar and polar solvents, as shown in Fig. 10.

This type of dependence confirms that the specific solvation of the dye molecules by polar solvents leads to the fluorescence quenching [58]. Fluorescence quenching in chloroform can be caused by interactions of the hydrogen atoms of chloroform molecules with nitrogen atoms of helicand anions.

In the electron-donating solvents the extra coordination of solvent molecules by metal ions and the formation of complex solvates $[M_2L_2(Solv)_n]$ are possible as it was previously found for structurally related dipyrrinates $[M(dpm)_2]$ [59], and the metalloporphyrins [60]. The process of extra coordination proceeds easier on the excited $[M_2L_2]$ molecules, in which the electron density on the nitrogen atoms and the metal is changed. This causes an increase in the probability of nonradiative transitions.

In this regard, the dependence of fluorescence quantum yield of $[Zn_2(\mathbf{11})_2]$ complex on the composition of binary mixtures of nonpolar and polar solvents was studied (Fig. 11).

In cyclohexane–alcohol and benzene–alcohol mixtures the value of Φ_f is reduced by 2 and 100 times at the mole fraction of the polar component χ ~0.1–0.15 and more than 0.5, respectively. Significant decrease of fluorescence intensity in the system benzene–dimethylsulfoxide is observed. In this system, the value of Φ_f is reduced by two-fold already at χ(dimethylsulfoxide) $\approx$0.04. Thus, for all studied systems the main changes of Φ_f are observed at low ($\chi < 0.15$) additive of the polar component, which is characteristic of specific interactions in the solvation shell of excited fluorophore [58].

High selectivity is an important feature of the behaviour of $[Zn_2L_2]$ complexes compared to BF_2-dipyrromethene dyes [25], and is of interest for the development of optical sensors for the presence of polar electron-donor and proton-donor molecules.

2.2.3. The temperature effect

It is known that the distance between interacting atoms in molecules and their mobility in an excited state can be changed by freezing of compounds/matrix. Therefore, the dependence of the fluorescence of the complexes $[Zn_2(\mathbf{11})_2]$–$[Zn_2(\mathbf{14})_2]$ in ethanol and cyclohexane on the temperature was investigated [53]. The fluorescence intensity of $[Zn_2L_2]$ complexes in frozen (77 K) cyclohexane is retained the same as at room temperature with a slight blue shift (5–8 nm) of the emission band. As shown in Fig. 12(A), when $[Zn_2(\mathbf{12})_2]$ ethanol solutions are cooled from 300 to 77 K, similar shift of the emission maximum is observed and fluorescence quantum yield increases in 100 times as compared to alcoholic solutions at 298 K. The fluorescence quantum yield of the $[Zn_2(\mathbf{12})_2]$ alcohol solution at 77 K is equal to Φ_f for $[Zn_2(\mathbf{12})_2]$ in cyclohexane at 298 K.

2.2.4. Long-lived (millisecond) radiation spectra

Long-lived (millisecond) radiation spectra of frozen $[Zn_2(\mathbf{12})_2]$ in ethanol and cyclohexane solutions has the same bands with small displacement and a redistribution of the intensities in them (Fig. 12(B)) [53]. The band with a maximum at 750 nm and a lifetime of 26 ms was attributed to phosphorescence, which is confirmed by the coincidence of the excitation spectra of the phosphorescence in this band and the absorption spectra of the complex (Fig. 12(C)). The most intense band in the long-lived radiation spectrum coincides with usual fluorescence

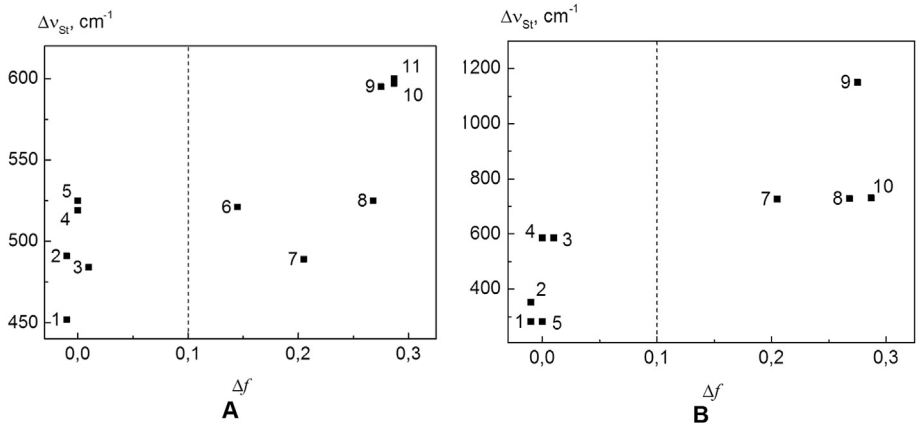

Fig. 10. The dependence of Stokes shift ($\Delta\nu_{St}$) of $[Zn_2(\mathbf{11})_2]$ (A) and $[Zn_2(\mathbf{20})_2]$ (B) on universal interactions function (Δf) of the solvent: *1* – cyclohexane, *2* – hexane, *3* – toluene, *4* – benzene, *5* – heptane, *6* – chloroform, *7* – tetrahydrofuran, *8* – 1-propanol, *9* – dimethylformamide, *10* – ethanol, *11* – acetone [53].

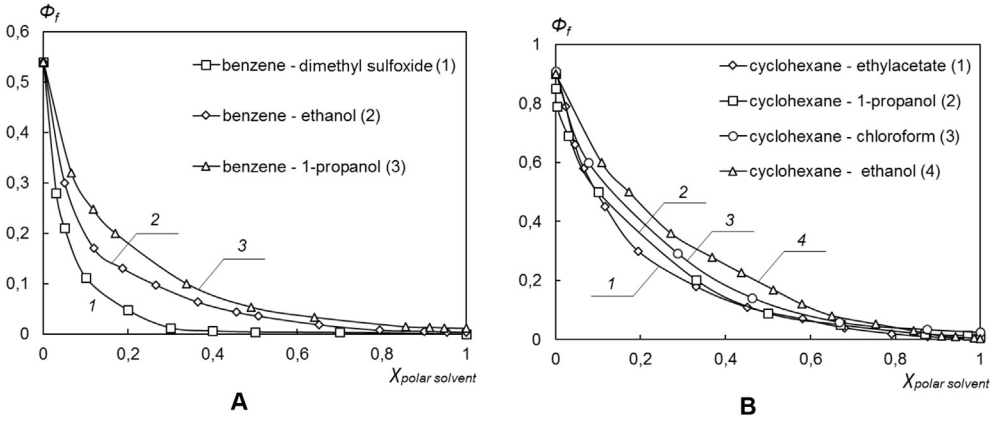

Fig. 11. The dependence of $[Zn_2(\mathbf{11})_2]$ helicate fluorescence quantum yield (Φ_f) in binary solvents based on the of cyclohexane (A) and benzene (B) on the mole fraction (χ) of cosolvent [54].

(λ_{max} = 540 nm) of $[Zn_2(\mathbf{12})_2]$ and connected with delayed fluorescence. Formation of delayed fluorescence occurs through the formation of an intermediate complex with radiation band about 650 nm.

Similar characteristics of long-lived radiation for ethanol and cyclohexane solutions and significant increase in fluorescence intensity of frozen $[Zn_2L_2]$ ethanol solutions are the result of a substantial reduction in structural "transformations". The effect of the temperature dependence on the fluorescence yield of ethanol solutions of the complexes is of interest to control of the temperature (in the range 300–80 K), which is important in the development a simple and visual ways to control the temperature in cryostats, etc.

2.2.5. Generation of stimulated emission

Since the results on the lasing characteristics of complexes such as dipyrrinates and bis(dipyrrinate)s were absent in the literature, the possibility of the generation of stimulated emission of the $[Zn_2(\mathbf{11})_2]$ and $[Zn_2(\mathbf{14})_2]$ complexes upon excitation by the second harmonic of Nd:YAG laser (532 nm) has been studied [54]. Lasing, photochemical and resource characteristics of the studied complexes are presented in Table 5. Fig. 13(C) demonstrates the dependence of efficiency on the pump intensity for $[Zn_2(\mathbf{11})_2]$ and $[Zn_2(\mathbf{14})_2]$ complexes. It is found that $[Zn_2(\mathbf{11})_2]$–$[Zn_2(\mathbf{14})_2]$ solutions in cyclohexane generates stimulated emission (Fig. 13(A and B)) on the long-wavelength side of the fluorescence band (λ_{max}^{gen} = 552.5 nm for $[Zn_2(\mathbf{11})_2]$ and 559.5 nm $[Zn_2(\mathbf{12})_2]$) with low threshold ($\cong$0.5 MW × cm^{-2}). It can be seen that the efficiency is low, but the lasing thresholds are low (<1 MW × cm^{-2}), and there is quite narrow region of optimal pump levels. When increasing the intensity of the pump >10–15 MW × cm^{-2}, the efficiency value is decreased (Fig. 13(C)), which is apparently caused by reabsorption of radiation not only from the ground state, but also from the excited states.

The highest efficiency (11%) was obtained for the $[Zn_2(\mathbf{14})_2]$ complex with λ_{max}^{gen} = 560 nm. When increasing excitation density (W_{pump}) the decrease of generation efficiency for $[Zn_2(\mathbf{14})_2]$ complex (see Fig. 13(C)) was observed [54].

Under identical conditions of medium, the quantum yield of phototransformations of $[M_2L_2]$ depends on the ligand structure, but more significantly it increases with increasing of complex concentration (Table 5).

It should be noted that $[Zn_2(\mathbf{11})_2]$–$[Zn_2(\mathbf{14})_2]$ complexes are inferior to BODIPY in their generation efficiency. For example, the ethanolic solutions of commercial PM567 dye (Fig. 14) have higher (47%) values of the generation efficiency according to [61].

On the other hand, resource of laser media based of zinc(II) bis(dipyrrinate)s cyclohexane solutions is higher (P_{80} ~ 75 ÷ 120 J × cm^{-3}) than that for Rhodamine 6G solutions, which generates in this region of the spectrum with resource $P_{80}^{Rhodamine\ 6G}$ (2 × 10^{-4} M) = 70 J × cm^{-3}. Despite the low efficiency of laser media based on the studied complexes it should be noted that low threshold and fundamental feasibility of generation of

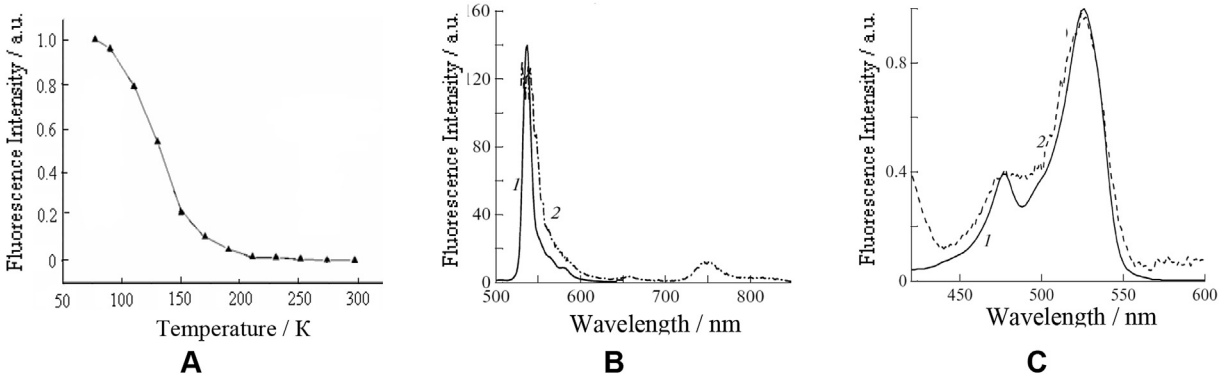

Fig. 12. The dependence of fluorescence intensity at the maximum of intense band of the $[Zn_2(\mathbf{12})_2]$ ethanol solution on the temperature: λ_{max}^{fl} = 544 nm (297 K), λ_{max}^{fl} = 539 nm (77 K) (77 K); λ_{ex} = 500 nm (A); fluorescence (*1*) and long-lived radiation (*2*) spectra of frozen (77 K) $[Zn_2(\mathbf{12})_2]$ ethanolic solution, λ_{ex} = 500 nm, the intensity of the spectrum *1* was reduced by 20 times (B). Normalized absorption spectra at room temperature (*1*) and excitation of phosphorescence at 77 K (*2*) of $[Zn_2(\mathbf{12})_2]$ in ethanol (registration wavelength (λ_{reg}) is 750 nm) (C) [53].

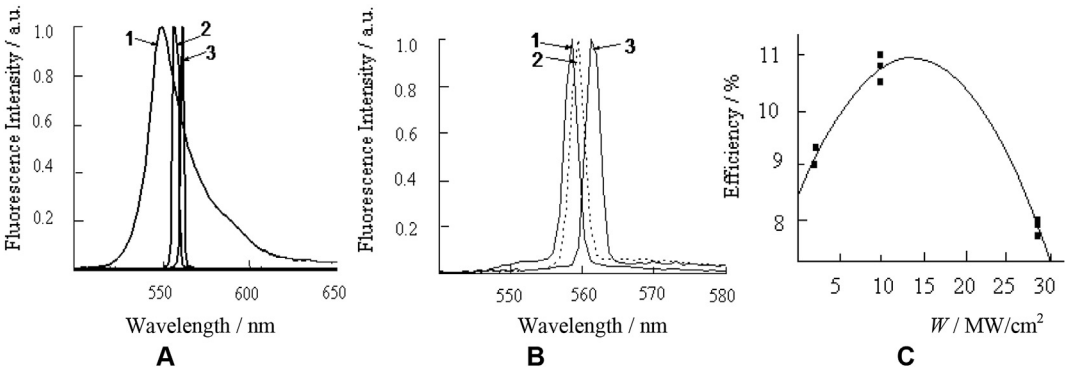

Fig. 13. Normalized fluorescence spectra of $[Zn_2(\mathbf{11})_2]$ in cyclohexane – *1* and generation spectra of $[Zn_2(\mathbf{11})_2]$ in cyclohexane – *2* (1×10^{-4} M), *3* (2×10^{-4} M) (A); generation spectra of $[Zn_2(\mathbf{14})_2]$ depending on the density of the pumping W_{pump}: 10 MW × cm^{-2} – *1*; 18 MW × cm^{-2} – *2*; 45 MW × cm^{-2} – *3* (B); dependence of the lasing efficiency (%) on the density of the pumping (λ_{pump} = 532 nm) for $[Zn_2(\mathbf{14})_2]$ ($c_{[Zn_2(14)_2]} = 2 \times 10^{-4}$ M) in cyclohexane (C) [54].

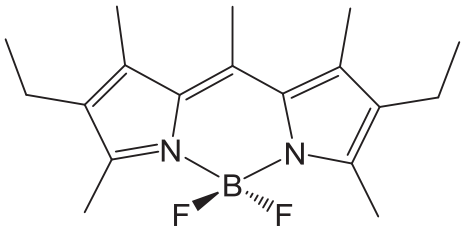

Fig. 14. PM567 dye structure formula [61].

stimulated emission by these complex structures and their good to adequate stability to the influence of the powerful pump radiation (Table 5).

2.2.6. Weakening of powerful pulsed radiation

The dependence of radiation transmission of the second and third harmonics of neodymium laser on the power density of lasing radiation (Fig. 15) was studied for $[Zn_2L_2]$ ethanolic solutions with weak fluorescence [53,54]. Transmission of second harmonic Nd:YAG laser is increased in the 10–50 MW × cm^{-2} region and decreases at high intensities (Fig. 14(B)). This fact is explained by a decrease of absorption in the S^0–S^1 band due to the transition of molecules in the excited state from which complexes absorb less efficiently at a given wavelength compared to the ground state. The third harmonic of Nd:YAG laser (355 nm) is attenuated in the entire range of intensities, which leads to a two-fold decrease of transmission power radiation (250–300 MW × cm^{-2}) (at an optical thickness of 5 mm, Fig. 14(A)) in agreement with the phosphorescence excitation spectrum (see Fig. 12(C)). These properties can be used to create limiters of powerful pulsed radiation.

2.2.7. Photodestruction of $[Zn_2L_2]$ complexes in solutions

The data on the photostability of $[Zn_2L_2]$ complexes are essential, since they characterize the resource of optical devices based on these dyes. It was established that the electronic spectrum of $[Zn_2L_2]$ solutions in aprotic organic solvents remains unchanged for six months or more when stored at light [55]. The photodestruction of $[Zn_2L_2]$ complexes in solution under the action of UV (355 nm) and visible (532 nm) laser radiation (2 and 3 harmonic of Nd:YAG laser) is manifested equally. As can be seen from Fig. 16 as a result of irradiation, the intensity of the wavelength bands is decreased and absorption in the near-and far-UV is enhanced [55]. The quantum yield of photodestruction process in cyclohexane (Φ_{photo}) in 4–5 times higher than that in ethanol (Table 5).

3. Conclusion

Dinuclear homoleptic $[M_2L_2]$ helicates of Co(II), Ni(II), Cu(II), Zn(II), Cd(II) and Hg(II) with bis(dipyrrin)s exhibit intense absorption (lgε ~5.00–5.52) in visible region of the spectrum (503–551 nm). $[Co_2L_2]$, $[Ni_2L_2]$ and $[Cu_2L_2]$ complexes are not fluorophores. The $[Zn_2L_2]$, $[Cd_2L_2]$ and $[Hg_2L_2]$ helicates give intense

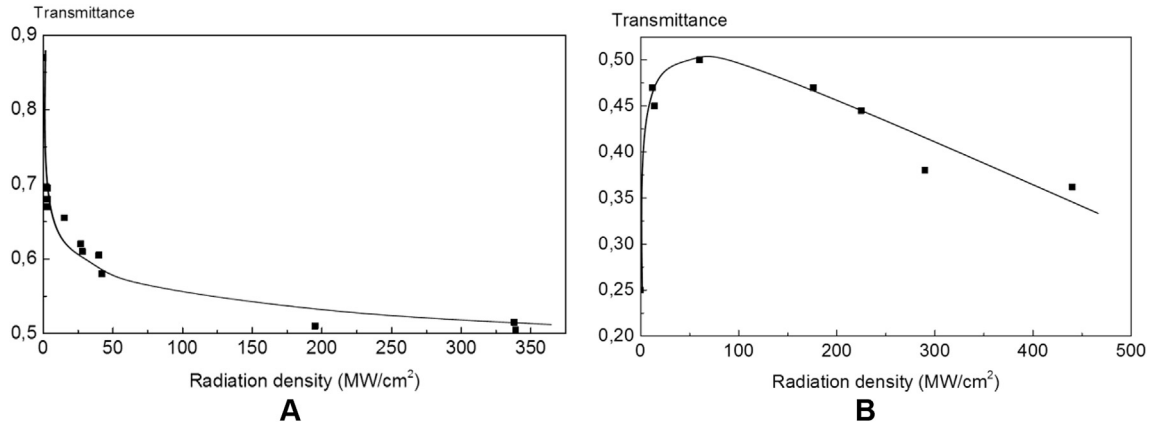

Fig. 15. The dependence of transmittance of the (A) third harmonic Nd:YAG laser, λ = 355 nm and (B) the second harmonic of Nd:YAG laser, λ = 532 nm for $[Zn_2(\mathbf{11})_2]$ ethanolic solution on the radiation density.[53,54].

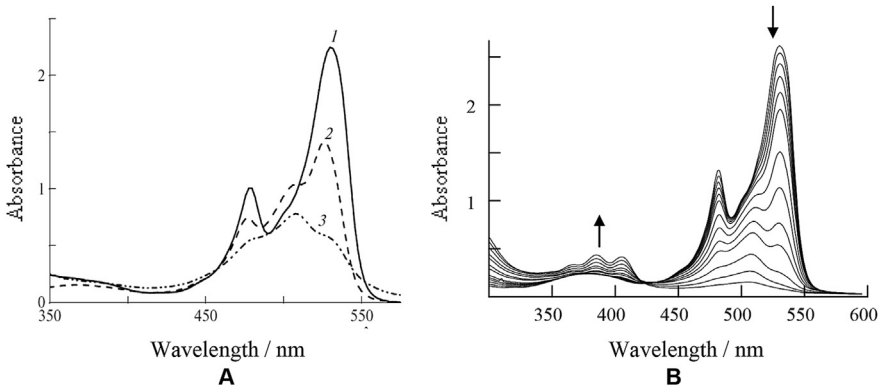

Fig. 16. The absorption spectrum of $[Zn_2(\mathbf{12})_2]$ in cyclohexane before irradiation – *1*, after irradiation in ethanol – *2* and in cyclohexane – *3* (λ_{irr} = 355 nm–*2*; 532 nm–*3*; W_{irr} = 60 MW × cm^{-2}), absorbed energy: 1.8 J × cm^{-3} – *2*; 13.4 J × cm^{-3} – *3* (A); spectral changes during the photodegradation of $[Zn_2(\mathbf{11})_2]$ in benzene under UV-irradiation (B) [55].

fluorescence in nonpolar solvents, comparable to fluorescence of boron dipyrromethene complexes. The fluorescence quantum yield of $[M_2L_2]$ helicates is increased in a series of 2,2′-, 2,3′-, 3,3′-bis(-dipyrrinate)s with the same type of complexing agent and in a series of $[Hg_2L_2]$ < $[Cd_2L_2]$ < $[Zn_2L_2]$ complexes with the same ligand almost in 30 times. The value fluorescence quantum yield reaches 0.99 for Zn(II) 3,3′-bis(dipyrrinate)s in saturated hydrocarbons solution. The fluorescence intensity of $[M_2L_2]$ is decreased almost by two-fold in aromatic solvents and becomes almost zero in the polar electron-donor media. The reason of fluorescence quenching is the specific solvation via extra coordination of electron-donor molecules, $\pi-\pi$ stacking and protonation of the nitrogen atoms of the ligand anions. These properties can be used in the development of fluorescent sensors of specifically solvating molecules.

Upon freezing and cooling of $[Zn_2L_2]$ ethanolic solutions from 300 to 77 K the value of fluorescence quantum yield of $[Zn_2L_2]$ is increased up to 100 times and becomes comparable with the quantum yield of $[Zn_2L_2]$ solutions in saturated hydrocarbons (at 298 K).

Temperature dependence of the fluorescence quantum yield of $[Zn_2L_2]$ is of interest in optical devices development for low temperatures monitoring. In nonpolar media $[Zn_2L_2]$ helicates generate stimulated emission in the 550–560 nm region when excited by the second harmonic of Nd:YAG laser with low threshold and good stability to the action of powerful pump radiation. Thereby for the first time the fundamental possibility obtaining of stimulated emission generation using open-chain oligopyrrolic coordination compounds was shown.

Acknowledgements

The work was supported by the Grant of the President of the Russian Federation No. MK-287.2014.3 (2014–2015); bursary of the President of the Russian Federation No. SP-6898.2013.4 for young scientists and graduate students engaged in advanced research and development in priority directions of modernization of the Russian economics (2013–2015); grant of the Russian Foundation for Basic Research (No. 12-03-97510-r_center_a); the grant of the Jewish agency for Israel and the government of Israel No. 1504994 (2014–2015).

References

[1] Fischer H, Orth H. Die Chemie des Pyrrols. Leipzig: Akademische Verlagsgesellschaft; 1937.
[2] Benstead M, Mehl GH, Boyle RW. 4,4′-Difluoro-4-bora-3a,4a-diaza-s-indacenes (BODIPYs) as components of novel light active materials. Tetrahedron 2011;67(20):3573–601.
[3] Awuah SG, You Y. Boron dipyrromethene (BODIPY)-based photosensitizers for photodynamic therapy. RSC Adv 2012;2(30):11169–83.
[4] Vendrell M, Krishna GG, Ghosh KK, Zhai D, Lee J-S, Zhu Q, et al. Solid-phase synthesis of BODIPY dyes and development of an immunoglobulin fluorescent sensor. Chem Commun 2011;47(29):8424–6.
[5] Boens N, Leen V, Dehaen W. Fluorescent indicators based on BODIPY. Chem Soc Rev 2012;41(3):1130–72.
[6] Wu Y, Peng X, Guo B, Fan J, Zhang Zh, Wang J, et al. Boron dipyrromethene fluorophore based fluorescence sensor for the selective imaging of Zn(II) in living cells. Org Biomol Chem 2005;3:1387–92.
[7] Sunahara H, Urano Y, Kojima H, Nagano T. Design and synthesis of a library of BODIPY-based environmental polarity sensors utilizing photoinduced electron-transfer-controlled fluorescence ON/OFF switching. J Am Chem Soc 2007;129(17):5597–604.
[8] Wang D, Fan J, Gao X, Wang B, Sh Sun, Peng X. Carboxyl BODIPY dyes from bicarboxylic anhydrides: one-pot preparation, spectral properties, photostability, and biolabeling. J Org Chem 2009;74(20):7675–83.
[9] Gorman A, Killoran J, O'Shea C, Kenna T, Gallagher WM, O'Shea DF. In vitro demonstration of the heavy-atom effect for photodynamic therapy. J Am Chem Soc 2004;126(34):10619–31.
[10] Lee CY, Farha OK, Hong BJ, Sarjeant AA, Nguyen S-BT, Hupp JT. Light-harvesting metal–organic frameworks (MOFs): efficient strut-to-strut energy transfer in bodipy and porphyrin-based MOFs. J Am Chem Soc 2011;133(40):15858–61.
[11] Lee JS, Kim HK, Feng S, Vendrell M, Chang Y-T. Accelerating fluorescent sensor discovery: unbiased screening of a diversity-oriented BODIPY library. Chem Commun 2011;47:2339–41.
[12] Ganja VA, Gurinovitch GP, Dzhagarov BM, Shulga AM, Nizams AN. Primary photoprocesses in dipyrrolylmethenes. Zh Appl Spectrosc 1987;47(1):84–7.
[13] Sazanovich IV, Kirmaier Ch, Hindin E, Yu L, Bocian DF, Lindsey JS, et al. Structural control of the excited-state Dynamics of bis(dipyrrinato)zinc complexes: self-assembling chromophores for light-harvesting architectures. J Am Chem Soc 2004;126(9):2664–5.
[14] Thoi VS, Stork JR, Magde D, Cohen SM. Luminescent dipyrrinato complexes of trivalent group 13 metal ions. Inorg Chem 2006;45(26):10688–97.
[15] Sutton JM, Rogerson E, Wilson CJ, Sparke AE, Archibald SJ, Boyle RW. Synthesis and structural characterisation of novel bimetallic dipyrromethene complexes: rotational locking of the 5-aryl group. Chem Commun 2004:1328–9.
[16] Maeda H, Hashimoto T, Fujii R, Hasegawa M. Dipyrrin Zn^{II} complexes with functional aryl groups: formation, characterization, and structures in the solid state. J Nanosci Nanotechnol 2009;9(1):240–8.
[17] Song H, Rajendiran S, Koo E, Min BK, Jeong SK, Thangadurai TD, et al. Fluorescence enhancement of N_2O_2-type dipyrrin ligand in two step responding to zinc(II) ion. J. Luminescence 2012;132(11):3089–92.
[18] Ikeda Ch, Ueda S, Nabeshima T. Aluminium complexes of N_2O_2-type dipyrrins: the first hetero-multinuclear complexes of metallo-dipyrrins with high fluorescencequantum yields. Chem Commun 2009;18:2544–6.
[19] Sakamoto N, Ikeda Ch, Yamamura M, Nabeshima T. Structural interconversion and regulation of optical properties of stable hypercoordinate dipyrrin–silicon complexes. J Am Chem Soc 2011;133(13):4726–9.
[20] Kim H, Burghart A, Welch MB, Reibenspies J, Burgess K. Synthesis and spectroscopic properties of a new 4-bora-3a,4a-diaza-s-indacene (BODIPY®) dye. Chem Commun 1999:1889–90.
[21] Elliott PIP. Photophysical properties of metal complexes. Annu Rep Prog Chem Sect A 2010;106:526–52.
[22] Crawford SM, Al-Sheikh Ali A, Cameron TS, Thompson A. Synthesis and characterization of fluorescent pyrrolyldipyrrinato Sn(IV) complexes. Inorg Chem 2011;50(17):8207–13.

[23] Wood E, Thompson A. Advances in the chemistry of dipyrrins and their complexes. Chem Rev 2007;107(5):1831–61.
[24] Stork JR, Thoi VS, Cohen SM. Rare examples of transition-metal–main-group metal heterometallic metal–organic frameworks from gallium and indium dipyrrinato complexes and silver salts: synthesis and framework variability. Inorg Chem 2007;46(26):11213–23.
[25] Loudet A, Burgess K. BODIPY dyes and their derivatives: syntheses and spectroscopic properties. Chem Rev 2007;107(11):4891–932.
[26] Choi ShH, Kim K, Lee J, Do Y, Churchill DG. X-ray diffraction, DFT, and spectroscopic study of *N,N′*-difluoroboryl-5-(2-thienyl)dipyrrin and fluorescence studies of related dipyrromethanes, dipyrrins and BF_2-dipyrrins and DFT conformational study of 5-(2-thienyl)dipyrrin. Chem Crystallogr 2007;37(5):315–31.
[27] Kennedy DP, Kormos ChM, Burdette ShC. FerriBRIGHT: a rationally designed fluorescent probe for redox active metals. J Am Chem Soc 2009;131(24):8578–86.
[28] Ch Yu, Jiao L, Yin H, Zhou J, Pang W, Wu Y, et al. α-/β-formylated boron–dipyrrin (BODIPY) dyes: regioselective syntheses and photophysical properties. Eur J Org Chem 2011;28:5460–8.
[29] Baudron SA. Luminescent dipyrrin based metal complexes. Dalton Trans 2013;42:7498–509.
[30] Zhang Y, Wang Zh, Yan Ch, Li G, Ma J. Synthesis and self-assembly of a novel tetrapyrrole containing dipyrrin units linked at the 3,3′-positions. Tetrahedron Lett 2000;41(40):7717–21.
[31] Yang L, Zhang Y, Yang G, Chen Q, Ma JS. Zn(II) and Co(II) mediated self-assembly of bis(dipyrrin) ligands with a methylene spacer bridged at 3,3′-positions and their optical properties. Dyes Pigments 2004;62(1):27–33.
[32] Yang L, Zhang Y, Chen Q, Ma JS. Molecular rectangle formed by head-to-tail self-assembly of 1-(dipyrrin-2-yl)-19-(dipyrrin-3-yl)methane. Monatsh fur Chem 2004;135:223–9.
[33] Zhang Y, Thompson A, Rettig SJ, Dolphin D. The use of dipyrromethene ligands in supramolecular chemistry. J Am Chem Soc 1998;120(51):13537–8.
[34] Thompson A, Dolphin D. Double-helical dinuclear bis(dipyrromethene) complexes formed by self-assembly. J Org Chem 2000;65(23):7870–7.
[35] Thompson A, Dolphin D. Nuclear magnetic resonance studies of helical dipyrromethene–zinc complexes. Org Lett 2000;2(9):1315–8.
[36] Wood TE, Dalgleish ND, Power ED, Thompson A, Chen X, Okamoto Y. Stereochemically stable double-helicate dinuclear complexes of bis(dipyrromethene)s: a chiroptical study. J Am Chem Soc 2005;127(16):5740–1.
[37] Al-Sheikh-Ali A, Cameron KS, Cameron TS, Robertson KN, Thompson A. Highly diastereoselective templated complexation of dipyrromethenes. Org Lett 2005;7(21):4773–5.
[38] Al-Sheikh Ali A, Benson RE, Blumentritt S, Cameron TS, Linden A, Wolstenholme D, et al. Asymmetric synthesis of mono- and dinuclear bis(-dipyrrinato) complexes. J Org Chem 2007;72(13):4947–52.
[39] Khoury RG, Jaquinod L, Smith KM. Metal ion-induced self assembly of open-chain tetrapyrrole derivatives: double stranded dinuclear complexes from 10-oxo-5,15-biladienes. Tetrahedron 1998;54(11):2339–46.
[40] Zhang Zh, Dolphin D. A triple-stranded helicate and mesocate from the same metal and ligand. Chem Commun 2009:6931–3.
[41] Zhang Zh, Dolphin D. Synthesis of triple-stranded complexes using bis(dipyrromethene) ligands. Inorg Chem 2010;49(24):11550–5.
[42] Thompson A, Rettig SJ, Dolphin D. Self-assembly of novel trimers using dipyrromethene ligands. Chem Commun 1999:631–2.
[43] Ma L, Patrick BO, Dolphin D. Self-assembly of [2 × 2] grids and a hexagon using bis(dipyrrin)s. Chem Commun 2011;47:704–6.
[44] Antina LA, Guseva GB, V'yugin AI, Antina EV. Spectral and thermal properties of Zn(II), Co(II), Cd(II), Ni(II), Cu(II) and Hg(II) dinuclear double-helicates with 3,3′-bis(dipyrrolylmethene). Russ J Coord Chem 2012;38:529–36.
[45] Guseva GB, Antina LA, Antina EV, Vyugin AI. Thermal decomposition of dinuclear double-helical 3,3′-bis(dipyrrinato)zinc(II) complexes in air and argon. Thermochim Acta 2012;544(20):54–6.
[46] Antina LA, Guseva GB, V'yugin AI, Antina EV, Berezin MB. *meso*-Spacer influence on properties of zinc(II) complexes with 2,3′- and 3,3′-bis(dipyrrolylmethenes). Russ J Gen Chem 2013;83(6):1143–51.
[47] Berezin MB, Antina EV, Dudina NA, Bushmarinov IS, Antipin MYu, Antina LA, et al. Synthesis, structure and fluorescence of a zinc(II) chelate complex with bis(2,4,7,8,9-pentamethyldipyrrolylmethen-3-yl)methane. Mendeleev Commun 2011;21(3):168–70.
[48] Antina EV, Berezin MB, Dudina NA, Guseva GB, Antina LA, V'yugin AI. Synthesis and spectral properties of zinc(II) helicates with 3,3′-bis(dipyrrolylmethenes) series. Russ J Gen Chem 2010;80(6):1216–9.
[49] Antina LA, Dudina NA, Berezin MB, Guseva GB. Synthesis and spectral properties of helicate of cobalt(II) with bis(1,2,3,7,9-pentamethyldipyrrolylmethen-3-yl)methane. Russ J Gen Chem 2011;81(1):162–5.
[50] Antina LA, Dudina NA, Berezin MB, Guseva GB, Antina EV. Synthesis and spectral properties of the nickel(II) and mercury(II) helicates with 3,3′-bis(-dipyrrolylmethenes). Russ J Gen Chem 2011;81(3):591–4.
[51] Antina LA, Dudina NA, Guseva GB, Berezin MB, V'yugin AI. Synthesis and photophysical properties of Cd(II) and Cu(II) complexes with decamethylated bis(dipyrrolylmethene). Russ J Gen Chem 2011;81(11):2349–52.
[52] Antina LA, Guseva GB, V'yugin AI, Antina EV. Kinetics of the dissociation of zinc(II) complexes with 3,3′-bis(dipyrrolylmethenes) in acetic acid–benzene binary solvent. Russ J Phys Chem 2012;86(11):1639–46.
[53] Kuznetsova RT, Kopylova TN, Mayer GV, Sikorskaya OO, Ermolina EG, Guseva GB, et al. Photonics of zinc complexes of 3,3′-Bis(dipyrrolylmethenes). Opt Spectrosc 2011;110(3):385–93.
[54] Kuznetsova RT, Aksenova YuV, Orlovskaya OO, Kopylova TN, Telminiv EN, Mayer GV, et al. Study of photoprocesses in coordination compounds of zinc(II) and boron(III) with open-chain olygopyrroles for using in optical devices. High Energy Chem 2012;46:464–75.
[55] Kuznetsova RT, Maier GV, Sikorskaya OO, Lapin IN, Svetlichnyi VA, Antina LA, et al. Spectroscopy of the excited-state complex of Zinc(II) with 3,3′-bis(dipyrrolylmethene). High Energy Chem 2012;46(2):122–7.
[56] Milgrom LR. The colours of life: an introduction to the chemistry of porphyrins and related compounds. New York: Oxford Univ. Press; 1997. p. 249.
[57] Dudina NA, Antina EV, Guseva GB. Regularities of the formation of binuclear homo- and heteroleptic complexes of *d* metals with 3,3′-bis(dipyrrolylmethenes) in DMF. Russ J Coord Chem 2011;37(5):333–42.
[58] Lakowicz JR. Principles of fluorescence spectroscopy. New York and London: Plenum Press; 1983.
[59] Antina EV, Guseva GB, V'yugin AI. Peculiarities of the interspecies interactions of metallocomplexes of structurally similar α,α-dipyrrolylmethene and porphyrin with organic solvents. Russ J Phys Chem 2006;80(Suppl. 1):1–7.
[60] Ackarov KA, Berezin BD, Bystritskaya EV, Golubchikov OA, Koyfman OI, Kyz'mitsky VA, et al. Phorphyrins: spectroscopy, electrochemistry, application. Moscow: Nauka; 1987. p. 87.
[61] Mula S, Ray A, Banerjee M, Chaudhuri T, Dasgupta K, Chattopadhyay S. Design and development of a new pyrromethene dye with improved photostability and lasing efficiency: theoretical rationalization of photophysical and photochemical properties. J Org Chem 2008;73(6):2146–54.